

Adaptive Interval Model Control of Arc Welding Process

John Zhang and Bruce L. Walcott, *Senior Member, IEEE*

Abstract—The welding process is typically uncertain and its dynamics may vary with welding conditions. To control this process, robust algorithms such as the interval model control proposed by Zhang and Kovacevic (1997) are needed. To improve the response speed and system performance, the authors developed an adaptive interval model control system for keyhole plasma arc welding process in this study. The developed system identifies the process parameters online, converts the identification results to the intervals in Zhang and Kovacevic's algorithm (Zhang and Kovacevic 1997), and uses a prefilter to eliminate the effect of the keyhole process' fluctuation on the control system. Experiments comparing the adaptive interval model control system with its nonadaptive counterpart have been conducted to verify the effectiveness of the former in achieving fast response speed when the manufacturing conditions or the set-point vary.

Index Terms—Adaptive control, manufacturing, robustness, uncertain systems, welding.

I. INTRODUCTION

QUASI-KEYHOLE is a novel operation of plasma arc welding (PAW). In PAW, because of the constraining orifice [Fig. 1(a)], electrons emitted from the electrode flow through the ionized gas forming a highly constrained jet of arc plasma. The liquid metal melted by the arc forms a pool of liquid metal which is referred to as weld pool. The high pressure of the plasma jet can displace the liquid metal to generate a keyhole (deep narrow cavity surrounded by the weld pool liquid metal) as shown in Fig. 1(b). To minimize the heat input, the quasi-keyhole method has been proposed which keeps heating the metal work piece using a peak current until the keyhole is established but switches the current to the lower base level after the establishment of the keyhole is detected. As a result, the keyhole is closed and the heat input is maintained at a minimal level heat before the next cycle starts. To form continuous welds, the adjacent keyholes formed in different cycles must be overlapped. This requires the keyhole is established with a certain period of time. To this end, the peak current level must be sufficient. However, if peak current is too high, excessive arc pressure may blow liquid metal away from the weld pool even before the current is switched to the base level because the arc pressure is proportional to the square

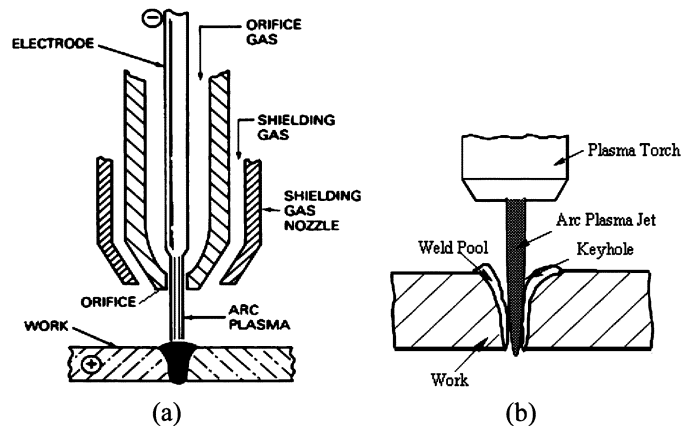


Fig. 1. Illustration of PAW torch and keyhole: (a) PAW Torch and (b) Keyhole.

of the current. Unfortunately, when manufacturing conditions change, the peak current required to establish a keyhole in a certain period also changes. Manufacturing applications, thus, demand a robust control system which can function properly under variations and fluctuations in manufacturing conditions or uncertain process models. Researchers at the University of Kentucky's Welding Research Laboratory have used adaptive control and nonlinear interval model control to control this process [1], [2]. In this brief, the authors use an adaptive method to online identify the parameters in an interval process model and then use the updated model to determine the needed peak current.

A number of publications have addressed adaptive control of welding processes. Song and Hardt [3] proposed an empirical discrete-time transfer function matrix model for gas metal arc welding process. Although the linearized model is valid only around the operating point of interest, the adaptation mechanism employed in the control system render this model useful over a wide operating range. Zhang *et al.* [4] used the adaptive generalized predictive control algorithm to control the weld profile measured by a structured-light vision system for gas tungsten arc welding. In [5], Leith and Leith used the gain-scheduling method to regulate the arc voltage in gas metal arc welding. Korizisand and Domanidis [6] implemented a single torch to sweep the joint surface by a controlled reciprocating motion. The welding temperature field was measured real-time by infrared temperature sensor and was fed back to a computer. An offline numerical simulation of the thermal field in scan welding was established, as well as a linearized multivariable model with real-time parameter identification. An adaptive thermal control scheme is, thus, conducted to ensure the composite morphologic, material and mechanical integrity of the joint. In [7], Santos and colleagues used adaptive predictive control method to control the trailing centerline's temperature in arc welding. Yamane and co-workers proposed an adaptive control

Manuscript received January 12, 2004; revised August 9, 2005. Manuscript received in final form May 10, 2006. Recommended by Associate Editor D. A. Schoenwald. This work was supported in part by the National Science Foundation under Grant DMI-0114982 and by the University of Kentucky under the Kentucky Young Research Scholarship Program.

J. Zhang was with the Department of Electrical and Computer Engineering, University of Kentucky, Lexington, KY 40506 USA. He is now with the Department of Electrical Engineering and Computer Science, Massachusetts Institute of Technology, Cambridge, MA 02139 USA (e-mail: czhang86@mit.edu).

B. L. Walcott is with the Department of Electrical and Computer Engineering, University of Kentucky, Lexington, KY 40506 USA (e-mail: walcott@enr.uky.edu).

Digital Object Identifier 10.1109/TCST.2006.880215

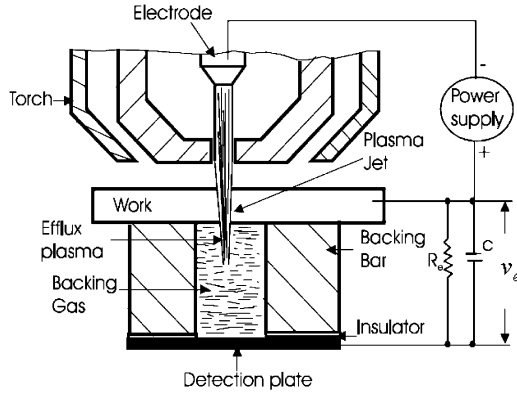


Fig. 2. Experimental setup.

for the weld bead on the backside in V groove welding without backing plate [8]. Recently, Zhang and Liu [1] developed an adaptive control system for the quasi-keyhole process. However, all the adaptive control systems aforementioned treated the process as a certain system and online identification was used to identify the parameters as exact values. Quantitative uncertainties were not used in the control algorithm design and the stability is not ensured. In this brief, the online identified uncertainties as measured by the parameter intervals are used to design the control algorithm and the stability is assured.

II. PROCESS

Fig. 2 shows the experimental setup. After the keyhole is established through the work piece, the efflux plasma generates a positive voltage v_e which is referred to as efflux plasma signal between the work piece and the metal detection plate in the chamber formed by the work piece, backing bar, and detection plate, and filled with backing gas. As can be seen in Fig. 3(a), at instant t_1 , the current is switched from base to peak current. The depths of the weld pool and the partial keyhole then increase under the peak current [Fig. 3(b)]. At t_2 , the weld pool becomes fully penetrated and the complete keyhole is established through the thickness of the work-piece [Fig. 3(b)]. This instant (t_2) can be detected using the efflux signal as the instant when the efflux signal exceeds the preset threshold. In general, the peak current is switched to the base current d , seconds ($d \geq 0$) after the establishment of the keyhole is confirmed. Denote this instant as t_3 , then the peak current duration $T_p = t_3 - t_1$. For the quasi-keyhole process, the current is switched back to the peak current at t_4 to start a new cycle after the base current is applied for a fixed period T_b . Denote the cycle from t_1 to t_4 as period k , then $T_p(k) = t_3 - t_1$ and $T_b(k) = t_4 - t_3$ [Fig. 3(a)]. The peak current I_p applied during $[t_1, t_3]$ was determined during period $k - 1$ and is, thus, denoted as $I_p(k - 1)$.

From controls point of view, the peak current I_p is adjusted as the control variable u to reduce or increase the time needed to establish the keyhole, thus, control the peak current period T_p as the output y . Table I lists the definition of the symbols which define the control system. The objective of this brief is to develop a robust control system in which the control variable u is adjusted to achieve the desired output $y^0 = T_p^*$ despite possible

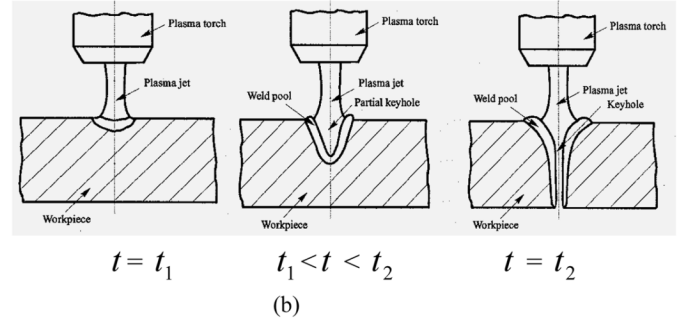
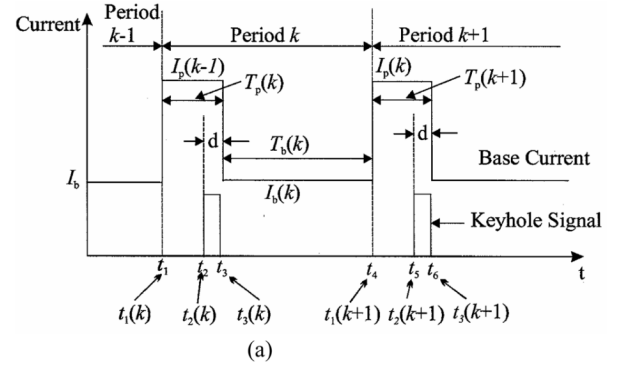


Fig. 3. Dynamic development in quasi-keyhole process: (a) Time sequence and (b) Keyhole and weld pool development.

TABLE I
NOTATIONS

Notation	Definition	Notation in system design
$I_p(k-1)$	Current applied during $[t_1, t_3]$ in period k	u_{k-1}
$T_p(k)$	$t_3 - t_1$, peak current duration in period k	y_k
$T_b(k)$	$t_4 - t_3$, base current duration in period k	N/A
$I_p(k)$	Current applied during $[t_4, t_6]$ in period $k+1$	u_k
$T_p(k+1)$	$t_6 - t_4$, peak current duration in period k	y_{k+1}

fluctuations/variations in manufacturing conditions. These variations include the standoff distance (the distance between the work piece and the plasma torch's orifice), the gap between the two pieces of metal to be welded, the flow rate of the orifice gas, etc.

III. ADAPTIVE INTERVAL MODEL CONTROL

An interval model is a useful description for parametric uncertainty. Abdallah *et al.* [9] and Olbrot and Nikodem [10] addressed a class of interval plants with one interval parameter. In [11], a prediction-based algorithm with guaranteed robust steady-state performance in tracking a given set-point is proposed by Zhang and Kovacevic to control interval plants described using a linear impulse response model with multiple independent intervals. This algorithm has been used to control the gas metal arc welding process [12].

A. Nonadaptive Interval Model Control

In the algorithm proposed by Zhang and Kovacevic in [11] for stable processes, the system is described using an impulse response model

$$y_k = \sum_{j=1}^n h(j)u_{k-j} \quad (1)$$

where k is the current instant, y_k is the output at k , and u_{k-j} is the input at $(k-j)$ ($j > 0$), while n and $h(j)$'s are the order and the real parameters of the impulse response function. Assume $h(j)$'s ($1 \leq j \leq n$) are time-invariant. They are unknown but bounded by the following intervals:

$$h_{\min}(j) \leq h(j) \leq h_{\max}(j) \quad (j = 1, \dots, n) \quad (2)$$

where $h_{\min}(j) \leq h_{\max}(j)$ are the known lower and upper bound of $h(j)$. Assume y^0 is the set-point. The objective is to design a controller for determining the feedback control actions $\{u_k\}$'s, so that the closed-loop system achieves

$$\lim_{k \rightarrow +\infty} y_k = y^0 \quad (3)$$

if $s_{\max}(n)s_{\min}(n) > 0$ (i.e., the sign of the static gain of the system is certain), where the upper and lower bounds of the static gain $s_{\max}(n)$ and $s_{\min}(n)$ can be directly obtained from the unit step response $s(i) = \sum_{j=1}^i h(j)$, i.e., $s_{\min}(n) = \sum_{j=1}^n h_{\min}(j)$ and $s_{\max}(n) = \sum_{j=1}^n h_{\max}(j)$.

Consider instant k ($k = 1, 2, 3, \dots$). Assume the feedback y_k is available and u_k needs to be determined. Model (1) yields

$$\Delta y_k = \sum_{j=1}^n h(j)\Delta u_{k-j} \quad (4)$$

where $\Delta y_k = y_k - y_{k-1}$ and $\Delta u_{k-j} = u_{k-j} - u_{k-j-1}$.

Based on (4), the following equation can be obtained to calculate the output at instant $k+i$ ($i > 0$) when the control actions are kept unchanged after instant k :

$$y_{k+i}|_{\Delta u_{k+j}=0(\forall j>0)} = y_k + \sum_{j=1}^n h(j) \sum_{l=1}^{\min(i,j)} \Delta u_{k+l-j} \quad (i = 1, 2, 3, \dots). \quad (5)$$

For simplification, denote $y_{k+i}|_{\Delta u_{k+j}=0(\forall j>0)} = y_{k+i}(\Delta u_k)$. When $i = n$, (5) results in

$$y_{k+n}(\Delta u_k) = y_k + \sum_{j=2}^n h(j) \sum_{l=1}^{j-1} \Delta u_{k+l-j} + \sum_{j=1}^n h(j)\Delta u_k. \quad (6)$$

Hence

$$y_{k+n}(\Delta u_k) = y_k + \sum_{j=2}^n h(j)f(j, \Delta U_{k-1}) + s(n)\Delta u_k \quad (7)$$

where ΔU_{k-1} represents the knowledge of $(\Delta u_{k-1}, \Delta u_{k-2}, \dots)$, and $f(j, \Delta U_{k-1}) = \sum_{l=1}^{j-1} \Delta u_{k+l-j} = u_{k-1} - u_{k-j}$. It is evident

$$\begin{aligned} y_{k+n}(\Delta u_{k-1}) &= y_{k+n}(\Delta u_k)|_{\Delta u_k=0} \\ &= y_k + \sum_{j=2}^n h(j)f(j, \Delta U_{k-1}). \end{aligned} \quad (8)$$

Thus

$$y_{k+n}(\Delta u_k) = y_{k+n}(\Delta u_{k-1}) + s(n)\Delta u_k. \quad (9)$$

The control action Δu_k is so determined that

$$\max y_{k+n}(\Delta u_k) = \max y_{k+n}(\Delta u_{k-1}) + \max(s(n)\Delta u_k) = y^0 \quad (10)$$

It is evident that the control algorithm given by (10), can also be written as

$$\begin{aligned} \max(s(n)\Delta u_k) &= y^0 - y_k - \sum_{j=2}^n \max(h_{\min}(j)f(j, \Delta U_{k-1}), \\ &\quad h_{\max}(j)f(j, \Delta U_{k-1})). \end{aligned} \quad (10a)$$

It has been proven by Zhang and Kovacevic [11] that the closed-loop system is stable and $\lim_{k \rightarrow +\infty} y_k = y^0$ if $h_{\min}(j) \leq h(j) \leq h_{\max}(j)$ ($j = 1, \dots, n$) and $s_{\max}(n)s_{\min}(n) > 0$ when algorithm (10) or (10a) is used.

B. Adaptive Interval Model Control

The algorithm assumes that the system to be controlled is described by (1) and (2). For identification purposes, this model becomes cumbersome due to the large number of parameters. To minimize the number of parameters needing identification, a model with autoregression of the form

$$y_k = a_1 y_{k-1} + a_2 y_{k-2} + \dots + a_p y_{k-p} + b_1 u_{k-1} + \dots + b_q u_{k-q} \quad (11)$$

may be used. In an earlier study [13], the authors developed a general method to convert the intervals of α_1, α_2 , and b_1 in the second-order model $y_k = a_1 y_{k-1} + a_2 y_{k-2} + b_1 u_{k-1}$ whose transfer function is

$$H(z) = \frac{b_1 z^{-1}}{1 - a_1 z^{-1} - a_2 z^{-2}} = \frac{b_1 z^{-1}}{(1 - \alpha_1 z^{-1})(1 - \alpha_2 z^{-1})} \quad (12)$$

into the intervals in (1). That particular study established the foundation to use the interval model control algorithm adaptively. When α_1 and α_2 are real and distinctive as will be in this brief

$$H(z) = h(1)z^{-1} + h(2)z^{-2} + h(3)z^{-3} + \dots \quad (13)$$

where

$$h(j) = b_1 c_1 \alpha_1^{j-1} + b_1 c_2 \alpha_2^{j-1} = \frac{b_1(\alpha_1^j - \alpha_2^j)}{\alpha_1 - \alpha_2} \quad (j = 1, 2, 3, \dots) \quad (14)$$

and

$$\begin{cases} c_1 = 1/(1 - \alpha_2/\alpha_1) = \alpha_1/(\alpha_1 - \alpha_2) \\ c_2 = 1/(1 - \alpha_1/\alpha_2) = -\alpha_2/(\alpha_1 - \alpha_2). \end{cases} \quad (15)$$

In this case, (14) can be written as

$$h(j) = b_1(\alpha_1^{j-1} + \alpha_1^{j-2}\alpha_2 + \alpha_1^{j-3}\alpha_2^2 + \dots + \alpha_2^{j-1}) \quad (j = 1, 2, 3, \dots). \quad (14A)$$

Because b_1 is independent from α_1 , and α_2 , $h_{\max}(j)$ and $h_{\min}(j)$ will occur at four possible locations

$$\begin{aligned} &(b_{1 \min}, \min f(\alpha_1, \alpha_2)), & (b_{1 \min}, \max f(\alpha_1, \alpha_2)) \\ &(b_{1 \max}, \min f(\alpha_1, \alpha_2)), & (b_{1 \max}, \max f(\alpha_1, \alpha_2)) \end{aligned}$$

where $f(\alpha_1, \alpha_2) = \alpha_1^{j-1} + \alpha_1^{j-2}\alpha_2 + \alpha_1^{j-3}\alpha_2^2 + \dots + \alpha_2^{j-1}$. To find $\min f(\alpha_1, \alpha_2)$ and $\max f(\alpha_1, \alpha_2)$, an analytic method has been developed that divides the possible distinct real pole interval combinations into three categories: 1) both positive; 2) both negative; and 3) differing polarities [13]. If both α_1 and α_2 are positive

$$f(\alpha_1, \alpha_2) = \alpha_1^{j-1} + \alpha_1^{j-2}\alpha_2 + \alpha_1^{j-3}\alpha_2^2 + \dots + \alpha_2^{j-1}. \quad (16)$$

Finding $\max f(\alpha_1, \alpha_2)$ and $\min f(\alpha_1, \alpha_2)$ with two positive α intervals is relatively straightforward. Positive α interval values guarantee positive values when exponentiated. To find $\max f(\alpha_1, \alpha_2)$, $\alpha_{1 \max}$ and $\alpha_{2 \max}$ will be used, i.e., $\max f(\alpha_1, \alpha_2) = f(\alpha_{1 \max}, \alpha_{2 \max})$. Similarly, using $\alpha_{1 \min}$ and $\alpha_{2 \min}$ will yield $\min f(\alpha_1, \alpha_2)$.

System parameters are identified online. System (12) can be expressed in the form $y(k) = \varphi^T(k)\theta$, where $\varphi(k) = [y(k-1) \ y(k-2) \ u(k-1)]^T$ and $\theta = [a_1 \ a_2 \ b_1]^T$. At every time instant k , $\varphi(k)$ changes, causing a change in θ . Although a number of effective algorithms exist, the recursive least-squares algorithm [14] is used

$$\hat{\theta}(k) = \hat{\theta}(k-1) + P(k)\varphi(k)(y(k) - \varphi^T(k)\hat{\theta}) \quad (17)$$

where $\hat{\theta}(k-1)$ is the previous θ and $P(k) = (\sum_{i=1}^k \varphi^T(i)\varphi(i))^{-1}$ can be calculated using a recursive algorithm.

After the parameters are identified online, they are converted into poles and pole intervals are acquired using history. The last m previous instants poles are searched and a maximum and minimum are found. Each instant yields a stable pair of parameters which can be converted into a pair of guaranteed stable poles. However, using history to obtain a pair of parameters does not guarantee a stable pair of parameters. Thus, we use history to obtain a pair of guaranteed stable poles.

IV. PROCESS MODEL

To determine the interval model for the keyhole plasma arc welding process, experiments have been performed at four "extreme" operating points for the manufacturing conditions in the range of interest. While many parameters can be kept constant, as given in Table II, the travel speed of the plasma torch and stand-off distance may vary from application to application or during manual operation. Therefore, the range of the manufacturing conditions is specified by the travel speed and stand-off distance. In this brief, the intervals of interest for the travel speed and stand-off distance are 1.8 mm/s, 2.7 mm/s and 5 mm, 8 mm,

TABLE II
CONSTANT WELDING PARAMETERS

Parameter	Value
Base current duration	420ms
Base current	30A
Pilot gas	2.8 L/min
Shielding gas	11.5 L/min
Efflux shielding gas	18.4 L/min
Diameter of orifice	2.4mm

respectively. These intervals are selected by considering common manufacturing specifications. Four sets of manufacturing conditions, as specified by the travel speed and stand-off distance, are used to conduct experiments in order to generate the input-output (I/O) data pairs for system identification. For each experiment, the input (peak current) is designed as a random number in an appropriate interval which can assure the establishment of the keyhole, thus, maintaining the process to be of quasi-keyhole. The interval of the peak current for each experiment is shown together with the resultant output (peak current duration) in Fig. 4.

It is found that the process can be modeled by

$$(y_k - y^{(0)}) = \alpha_1(y_{k-1} - y^{(0)}) + b_1(u_{k-1} - u^{(0)}) \quad (18)$$

using the operating point $(u^{(0)}, y^{(0)})$, or as

$$y_k = c_0 + \alpha_1 y_{k-1} + b_1 u_{k-1} \quad (19)$$

without using the operating point, where y is the output (peak current duration), u is the control variable or the input (peak current), (c_0, α_1, b_1) is the model parameter vector. Because the interval model control algorithm uses an incremental model, model (19) is used as the process model and it is equivalent to a transfer function

$$H_p(z) = b_1 z^{-1} / (1 - \alpha_1 z^{-1}). \quad (20)$$

Using the four sets of experimental data given in Fig. 4, four sets of parameter vectors are obtained based on the least-squares algorithm. They are

$$\begin{aligned} &(521, 0.4063, -3.4124), (385, 0.3524, -2.2879), \\ &(201.5, 0.3865, -1.06) \text{ and } (374, 0.1410, -1.8795) \end{aligned}$$

for experiments 1–4, respectively. The intervals for α_1 and b_1 are, thus, set at $\alpha_1 = [0.14, 0.41]$ and $b_1 = [-3.4, -1.0]$.

It is known [1] that the peak current duration fluctuates even when the peak current maintains at constant. This is because the establishment of the keyhole is a result of the balance among forces which govern the keyhole process and the fluctuation of fluid flow and, thus, the forces. Hence, the previous control system [1] used a penalty factor to restrict the variation in the control action. For the prediction-based interval model control algorithm, its prediction accuracy improves when the control variable is less fluctuating. Further, it appears the filtered output

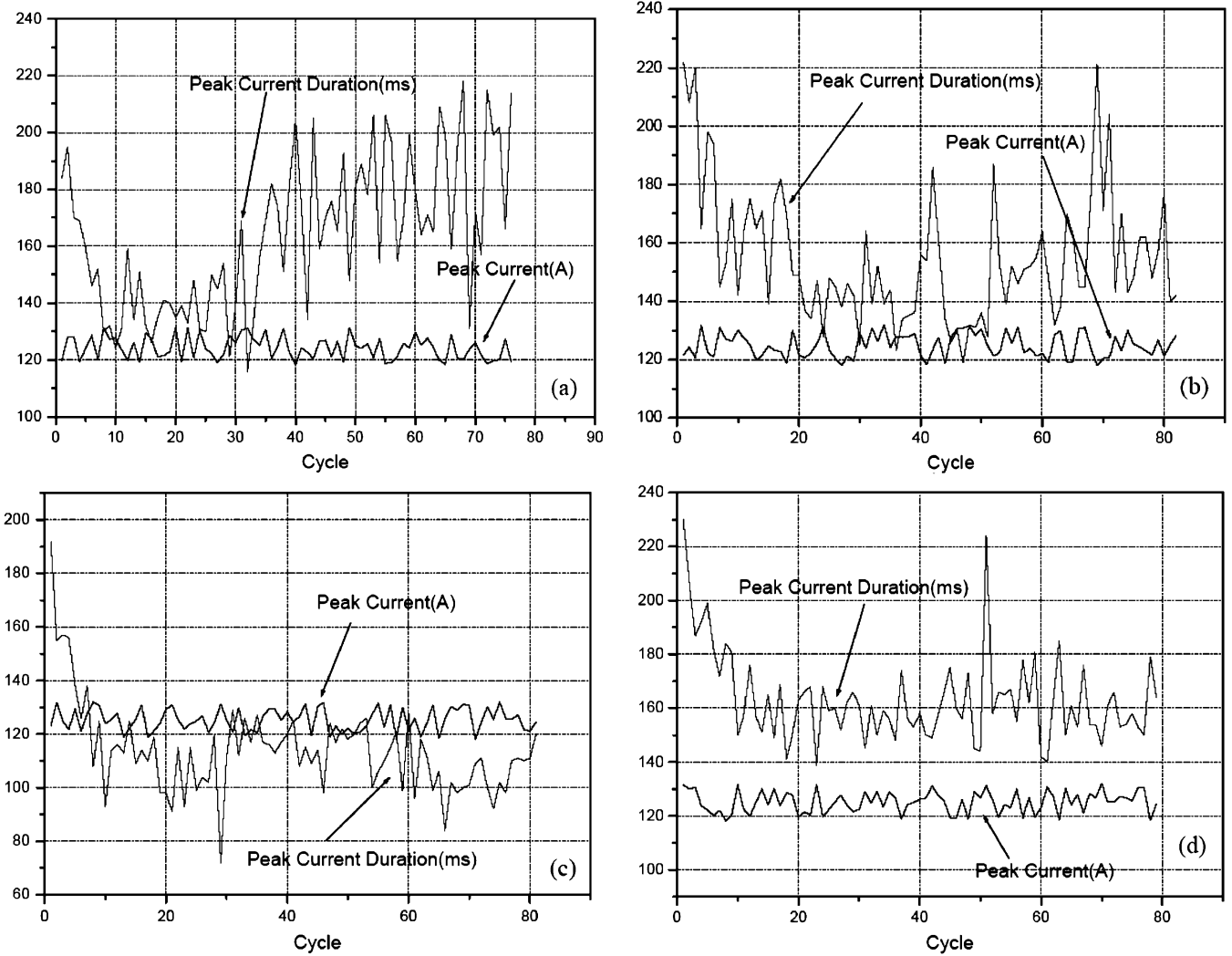


Fig. 4. System identification experiments. (a) Experiment 1: Stand-off distance = 6 mm, travel Speed = 2.7 mm/s. (b) Experiment 2: Stand-off distance = 7 mm, travel speed = 2.7 mm/s. (c) Experiment 3: Stand-off distance = 5 mm, travel speed = 1.8 mm/s. (d) Experiment 4: Stand-off distance = 8 mm, travel speed = 1.8 mm/s.

can better represent the state of the keyhole process. Hence, a prefilter $H_f(z)$ is used and the filtered output is used as the feedback in the control algorithm. The transfer function of the proposed prefilter is

$$H_f(z) = (1 - \alpha_2)/(1 - \alpha_2 z^{-1}). \quad (21)$$

Its static gain [15] is $(1 - \alpha_2)/(1 - \alpha_2) = 1$. As a result, the model of the controlled process becomes

$$H(z) = H_p(z)H_p(z) = b_1 z^{-1}/(1 - \alpha_1 z^{-1})(1 - \alpha_2 z^{-1}). \quad (22)$$

Although α_2 is fixed as a design parameter, the intervals can still be determined for $(\alpha_1, \alpha_2, b_1)$ and be applied to conduct the needed interval conversion. It is found that $\alpha_2 = 0.9$ gives very slow response and $\alpha_2 = 0.8$ can compromise the response speed with the inherent fluctuation of the keyhole process to generate good control performance as will be shown in the closed-loop control experiments.

V. EXPERIMENTS

To test the developed adaptive interval control algorithm for keyhole process, experiments have been implemented. The *a priori* intervals are determined by finding the parameters that best fit previous offline identification experimental data ($\alpha_1 : [0.14, 0.41]$, $\alpha_2 : [0.8, 0.8]$, $b_1 : [-3.4, -1.0]$). During welding/control experiments, the beginning 27 cycles are open-loop controlled using random peak current. (The range of the random peak current has been designed to assure the keyhole can be established although the peak current duration is not controlled.) During this initial period, the process's parameters are online identified but not used by the control algorithm to calculate the peak current. The intervals at each cycle are determined using the identification results in the previous 20 cycles, i.e., $m = 20$. When the closed-loop control begins at cycle 28, the online identified intervals are compared with the *a priori* intervals. If the online identified intervals lie in the *a priori* intervals, the online identified intervals are used to implement the adaptive interval model control. Otherwise, the *a priori* intervals are used.

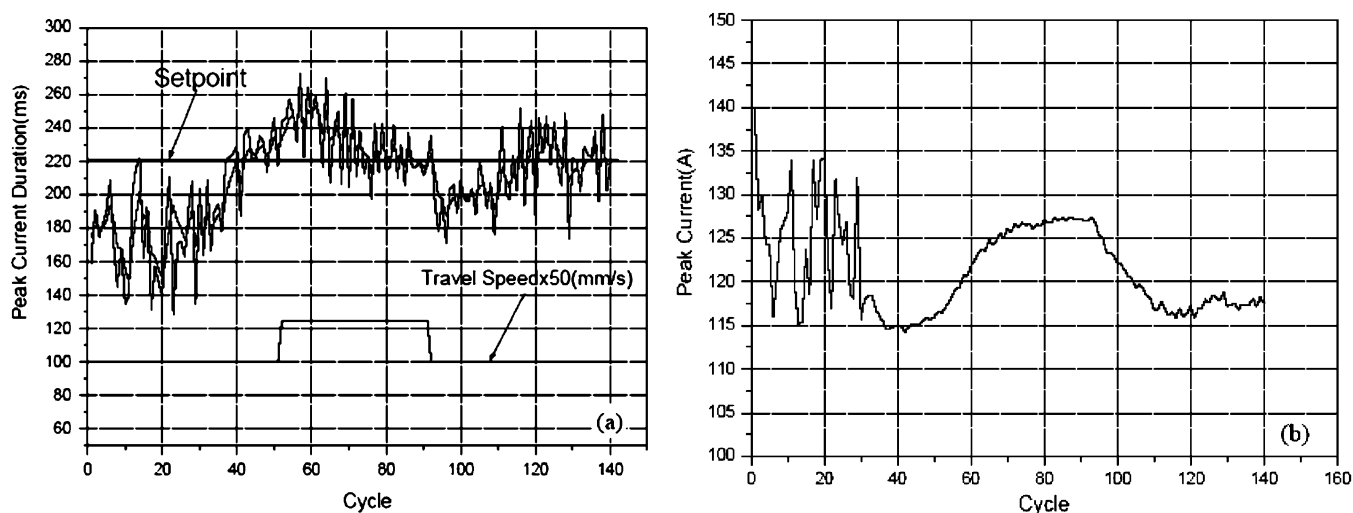


Fig. 5. Adaptive interval model control under varying welding speed. (a) Peak current duration. (b) Peak current.

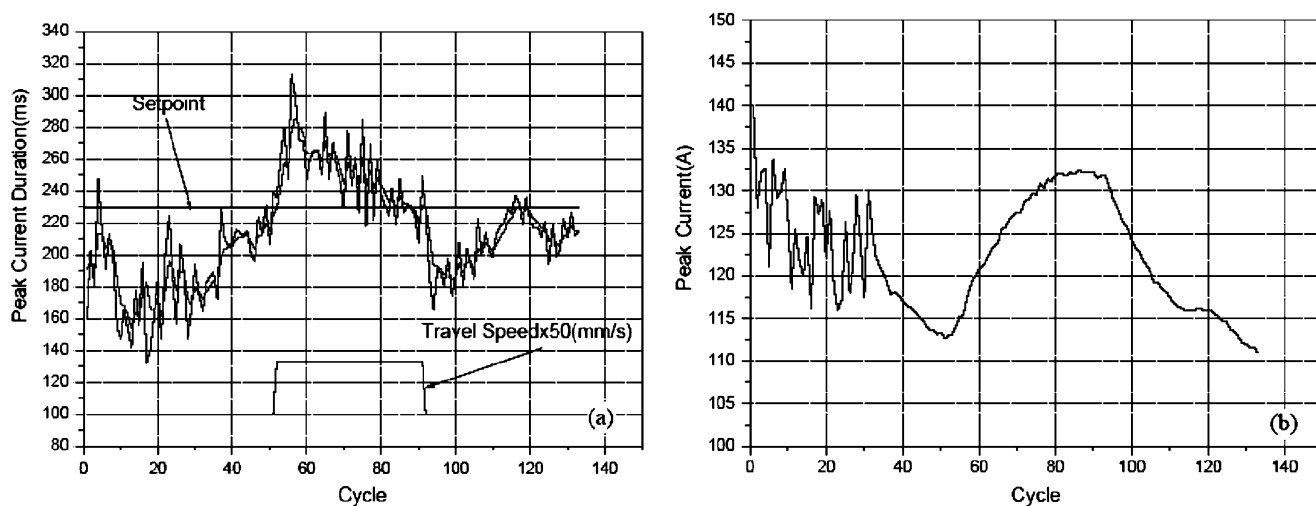


Fig. 6. Nonadaptive interval model control under varying welding speed. (a) Peak current duration. (b) Peak current.

Two types of experiments have been done. In experiment (type) 1, the desired peak current duration was set to 420 ms. The orifice diameter of the plasma arc welding nozzle was 2.4 mm. The welding speed varied to provide variations in manufacturing conditions. The plasma gas and shielding gas flow rates were 2.8 and 11.5 L/min, respectively. Welding experiments were fulfilled on stainless steel 304-plate with the thickness of 3.3 mm. The prefilter was used to block out the effect of the fluctuation of the keyhole process on control system. Fig. 5 gives the results using the adaptive interval model. For comparison, the results associated with the nonadaptive interval model control system are plotted in Fig. 6.

For both adaptive and nonadaptive control trials, at cycle 28, feedback control begins. There is a 10-ms difference between the set points of the adaptive and nonadaptive trials. Despite this difference, it is obvious the adaptive algorithm completed the initial adjustment and reached the set point faster at cycle 35. The peak current after cycle 35 and before the speed change at cycle 50, did not adjust significantly. However, as can be seen in Fig. 6, the nonadaptive algorithm did not com-

plete the initial adjustment before the speed was changed at cycle 50.

After the speed has its first change at cycle 50, the adaptive system takes approximately 20 cycles to complete the readjustment as can be seen in Fig. 5(a) and (b). However, the nonadaptive system took 30 cycles to complete the readjustment. The similar phenomenon was observed after the speed had its second change at cycle 90. Again the adaptive system took 20 and the nonadaptive took 30 cycles to complete the corresponding adjustment. Further, after cycle 120, the output dropped in the nonadaptive trial. It appears that this drop could have been avoided if the nonadaptive control could be smart enough to not stop the peak current's decrease so quickly. Because of this "mistake," the peak current duration did not resume back to the set-point before the welding ended. It is believed that the large intervals should be responsible for the relatively poor performance of the nonadaptive system in comparison with the adaptive system.

A second type of experiments was run to test the relative performance of the adaptive and nonadaptive interval model

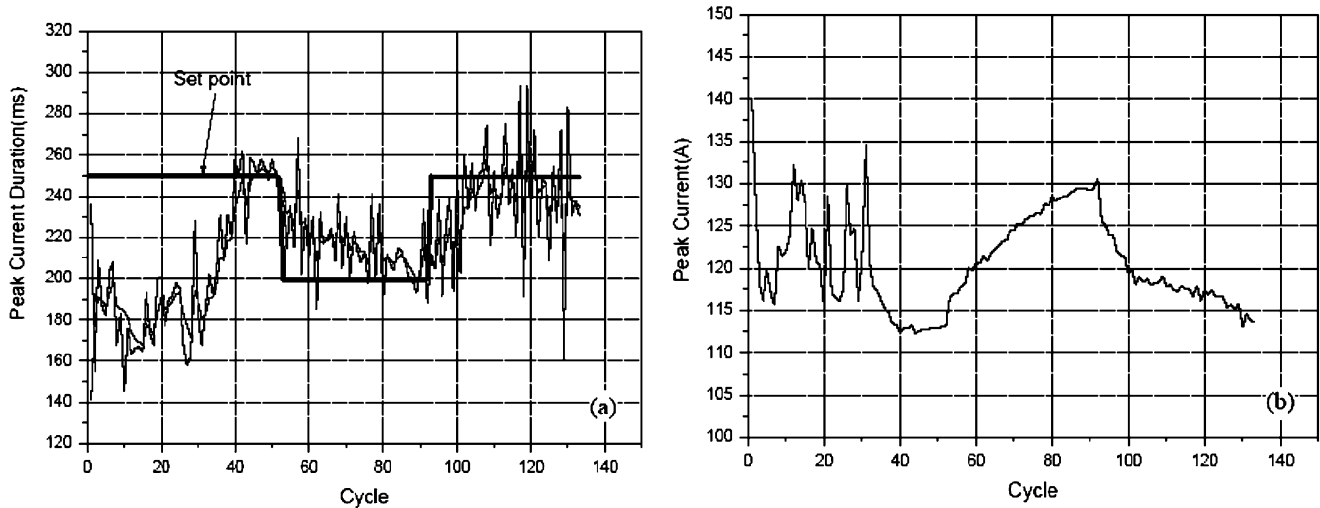


Fig. 7. Adaptive interval model control under varying set-point. (a) Peak current duration. (b) Peak current.

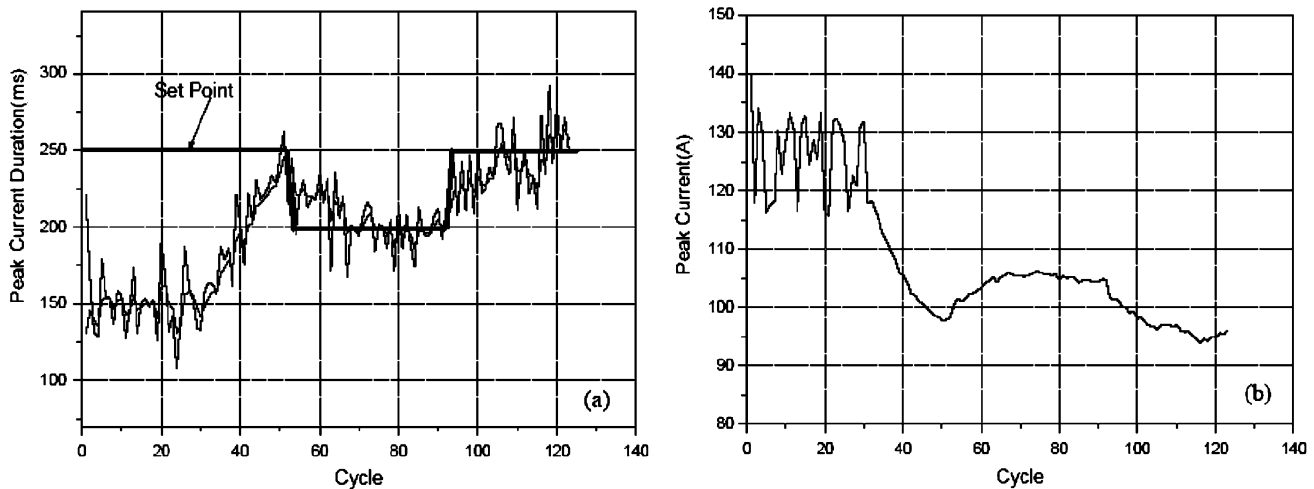


Fig. 8. Nonadaptive interval model control under varying welding speed. (a) Peak current duration. (b) Peak current.

control algorithms with a changing set point. In experiment (type) 2, the desired peak current duration was initially set to 250 ms. The orifice diameter of the plasma arc-welding nozzle was 2.4 mm. The welding speed is 2.22 mm/s. The plasma gas and shielding gas flow rates were 2.8 and 11.5 L/min, respectively. Welding experiments were fulfilled also on stainless steel 304-plate with the thickness of 3.3 mm. The set point changed at cycles 50 and 90.

Figs. 7 and 8 depict the results for the adaptive and nonadaptive control trials, respectively. For both trials, at cycle 28, the feedback control begins. At cycle 50, the set point is lowered from 250 to 200 ms. At cycle 90, the set point rises again to 250 ms. Again, as can be seen in Figs. 7 and 8, the adaptive system completed its initial adjustment approximately at cycle 40 but the nonadaptive system took 10 more cycles to complete the initial adjustment. When the set point was lowered to 200 ms, it appears that the adaptive control system took much longer to complete the adjustment. However, a closer look at Figs. 7(b) and 8(b) shows that the change of the peak current associated with this adjustment was approximately 17 A for the adaptive trial. However, for the nonadaptive trial, the change

of the peak current was only approximately 7 A. This implies that the actual conditions for the two trials were not exactly the same. Hence, the much longer adjustment time associated with the adaptive trial does not imply that the performance of the adaptive system is less desirable. Moreover, the adjustment of the peak current in the adaptive trial was much faster and no overshoot resulted. Hence, the adaptive system is still superior. The similar phenomenon was also observed after the set-point increased at cycle 90 from 200 to 250 ms. Again, in 10 cycles (from 90 to 100), the peak current decreased 12 A during the adaptive trial. However, the nonadaptive system only decreased the peak current approximately 6 A.

VI. CONCLUSION

This brief developed an adaptive interval model control system to control the keyhole plasma arc welding process. Experiments were conducted to identify the *a priori* intervals of the parameters. During welding, parameter intervals were online identified and used in the interval model control algorithm if lying in the *a priori* intervals. A prefilter was used to suppress the inherent fluctuation of the keyhole process on

control system. Experiments have shown that the developed adaptive interval model control system does provide faster response and better performance over the nonadaptive control system.

ACKNOWLEDGMENT

One of the authors, J. Zhang, would like to thank Y. Liu and W. Lu at the Welding Research Laboratory for their assistance with the experiments.

REFERENCES

- [1] Y. M. Zhang and Y. C. Liu, "Modeling and control of quasi-keyhole arc welding process," *Contr. Eng. Practice*, vol. 11, pp. 1401–1411, 2003.
- [2] W. Lu, Y. M. Zhang, and W.-Y. Lin, "Nonlinear interval model control of quasi-keyhole arc welding process," *Automatica*, vol. 40, pp. 805–813, 2004.
- [3] J. B. Song and D. E. Hardt, "Dynamic modeling and adaptive-control of the gas metal arc-welding process," *Trans. ASME Dyn. Syst. Meas. Contr.*, vol. 116, pp. 405–413, 1994.
- [4] Y. M. Zhang, R. Kovacevic, and L. Li, "Adaptive control of full penetration gas tungsten arc welding," *IEEE Trans. Contr. Syst. Technol.*, vol. 4, no. 4, pp. 394–403, Jul. 1996.
- [5] D. J. Leith and W. E. Leithead, "On microprocessor-based arc voltage control for gas tungsten arc welding using gain scheduling," *IEEE Trans. Contr. Syst. Technol.*, vol. 7, no. 6, pp. 718–723, Nov. 1999.
- [6] G. Korizis and C. Doumanidis, "Scan welding: Thermal modeling and control of material processing," *Trans. ASME Manuf. Sci. Eng.*, vol. 121, pp. 417–424, 1999.
- [7] T. O. Santos, R. B. Caetano, J. M. Lemos, and F. J. Coito, "Multi-predictive adaptive control of arc welding trailing centerline temperature," *IEEE Trans. Contr. Syst. Technol.*, vol. 8, no. 1, pp. 159–169, Jan. 2000.
- [8] S. Yamane, H. Yamamoto, T. Ishihara, T. Kubota, K. Eguchi, and K. Oshima, "Adaptive control of back bead in V groove welding without backing plate," *Sci. Technol. Welding Joining*, vol. 9, pp. 138–148, 2004.
- [9] C. Abdallah, "Controller synthesis for a class of interval plants," *Automatica*, vol. 31, pp. 341–343, 1995.
- [10] A. W. Olbrot and M. Nikodem, "Robust stabilization: Some extensions of the gain margin maximization problem," *IEEE Trans. Autom. Contr.*, vol. 39, no. 3, pp. 652–657, Mar. 1994.
- [11] Y. M. Zhang and R. Kovacevic, "Robust control of interval plants: A time domain approach," *Inst. Elect. Eng. Proc. Contr. Theory Appl.*, vol. 144, pp. 347–353, 1997.
- [12] Y. M. Zhang, L. G. E., and B. L. Walcott, "Robust control of pulsed gas metal arc welding," *ASME J. Dyn. Syst. Meas. Contr.*, vol. 124, pp. 281–289, 2002.
- [13] C. Zhang and B. L. Walcott, "Adaptive interval model control and application," in *Proc. Amer. Contr. Conf.*, 2004, pp. 3185–3190.
- [14] L. Ljung, *System Identification-Theory for the User*, 2nd ed. Upper Saddle River, NJ: Prentice-Hall, 1997.
- [15] R. E. Ziemer, W. H. Tranter, and D. R. Fannin, *Signals & Systems: Continuous and Discrete*, 4th ed. Englewood Cliffs, NJ: Prentice-Hall, 1998.